

# Moiré versus Mott: Incommensuration and Interaction in One-Dimensional Bichromatic Lattices

DinhDuy Vu and S. Das Sarma

Condensed Matter Theory Center and Joint Quantum Institute,  
Department of Physics, University of Maryland, College Park, Maryland 20742, USA

Inspired by the rich physics of twisted 2D bilayer moiré systems, we study Coulomb interacting systems subjected to two overlapping finite 1D lattice potentials of unequal periods through exact numerical diagonalization. Unequal underlying lattice periods lead to a 1D bichromatic ‘moiré’ superlattice with a large unit cell and consequently a strongly flattened band, exponentially enhancing the effective dimensionless electron-electron interaction strength and manifesting clear signatures of enhanced Mott gaps at discrete fillings. An important non-perturbative finding is a remarkable fine-tuning effect of the precise lattice commensuration, where slight variations in the relative lattice periods may lead to a suppression of the correlated insulating phase, in qualitative agreement with the observed fragility of the correlated insulating phase in twisted bilayer graphene. Our predictions, which should be directly verifiable in bichromatic optical lattices, establish that the competition between interaction and incommensuration is a key element of the physics of moiré superlattices.

*Introduction* - Motivated by the intriguing and interesting recent experimental and theoretical studies observing correlated insulating phases in 2D moiré systems [1–4], we ask a simple conceptual question: Is there a one-dimensional analog for interacting moiré superlattices where correlated insulating phases manifest strongly in superlattices at fractional band fillings, but not in the corresponding original lattice? The advantage of asking this question in a 1D system is that the problem can be studied using exact numerical diagonalizations of finite size Coulomb interacting systems containing many unit cells of the superlattice, something completely out of question in 2D moiré systems because of the exponentially large Hilbert space sizes involved in two dimensions. In the current work, we provide detailed numerical results answering this question by focusing on electrons in a bichromatic 1D lattice with superposed periodic potentials with equal amplitudes, but differing lattice sizes, with the lattice size ratio defining the moiré superlattice through its rational fractional representation (see below). Our work establishes definitively that indeed correlated insulating phases emerge generically in such moiré superlattices, and in addition, we also show, as described and discussed in depth below, that the emergent correlated insulating phase is fragile, and may disappear under slight variations in the lattice period ratio because of a subtle competition between incommensuration and interaction. Our results, in addition to being of possible relevance to the observed correlated insulating phase in 2D moiré systems, should also be directly observable in 1D bichromatic atomic optical lattices [5–8]

*Model* - The model we study is a bichromatic 1D system with two overlapping periodic cosine potentials of periods  $a_1$  (which is taken to be the primary lattice) and  $a_2$ , with a long-range inter-particle Coulomb interaction. So, the single-particle lattice potential  $V(x)$  is given by  $V(x) = V_0 [\cos(2\pi x/a_1) + \cos(2\pi x/a_2)]$ . Here  $V_0 < 0$  is a

constant potential defining the lattice potential strength, and  $a_2/a_1 = m$  defines the moiré ratio of the combined potential. We take  $a_1/a_B = r_s$  as the dimensional lattice length, where  $a_B$  is the Bohr radius (all length is measured in units of Bohr radius and all energies in units of Hartree  $E_h = e^2/a_B$ ). The Coulomb interaction between the electrons at the locations  $x_i$  and  $x_j$  is given by  $V_{ij} = e^2/|x_i - x_j|$ . The system Hamiltonian is now defined by  $V(x) + V_{ij}$ , which we diagonalize exactly numerically for a system with  $N_e$  particles on a total system size of  $L = Na_1$  (i.e.  $N$  primary lattice sites) with free boundary conditions.

The ratio  $m = a_2/a_1$  is the key moiré superlattice parameter in our model, serving a role similar to the twist-angle  $\theta$  in twisted 2D moiré heterostructures (where two 2D layers are twisted by  $\theta$  with respect to each other to create the moiré pattern). While the unit cell size in the original lattice is  $a_1$ , in the moiré superlattice the unit cell size is increased to  $A = Ma_1 \gg a_1$ , where  $M$  is the lowest possible integer numerator in the rational fraction representation of  $m$ . For example, with  $a_2 = 1.4a_1$ ,  $1.5a_1$ ,  $1.6a_1$ , three examples used in this work,  $M = 7, 3, 8$  respectively, whereas for the original lattice ( $a_1 = a_2$ ),  $m = M = 1$ . The enhanced value of  $A$  compared with  $a_1$  leads to flat bands in the 1D superlattice very similar to what happens in 2D twisted systems (e.g. twisted bilayer graphene (tBLG)) [1–4].

*Results and Discussions* - In the rest of this paper, we now present and discuss our results for the 1D superlattice moiré states for  $m = 1.4, 1.5, 1.6$  cases, comparing with the original non-moiré situation of  $m = 1$ . Unless otherwise stated we choose  $V_0 = -3.5 E_h$ ,  $L = 63a_1$  (for noninteracting systems, we provide the exact band structure for infinite systems with periodic boundary conditions),  $N_e = 1 - 10$  (depending on the case as shown). We define  $V_c = e^2/A$  as the Coulomb coupling strength and  $t = (2A^2)^{-1} \partial^2 E(k) / \partial k^2$  at  $k = 0$  as the kinetic energy

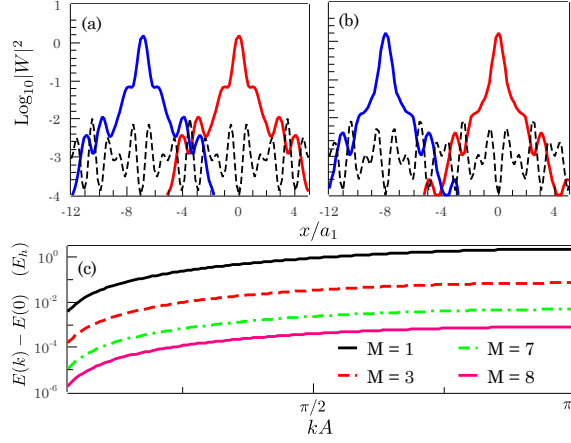


Figure 1. Squared amplitude  $|W|^2$  of two adjacent Wannier wavefunctions for (a)  $M = 7$  ( $m = 1.4$ ) and (b)  $M = 8$  ( $m = 1.6$ ). The dashed black lines are the total background potential including the original and the incommensurate lattice fields. (c) The lowest band dispersion as the function of the moiré momentum.

strength, thus providing  $V_c/t$  as the dimensionless interaction strength. Note that  $V_c/t$  depends on  $r_s = a_1/a_B$ , and  $V_c/t$  increases exponentially, for fixed  $r_s$ , with increasing  $A$  since  $t$  is suppressed exponentially, but  $V_c$  only as  $1/A$ , in the superlattice. We provide the calculated  $V_c/t$  values for each interacting situation we study in our results along with the values of  $m$  and  $M$  (for the noninteracting system  $V_c/t = 0$  by definition). Our results are mostly for  $r_s = 1$  unless otherwise stated explicitly. Note that  $r_s = 1$  indicates a situation (for the original lattice,  $a_1 = a_B$ ) which is of intermediate coupling strength since the strong coupling regime is defined by  $r_s \gg 1$ . We note that the values of  $r_s$  and  $V_c/t$  are inferred quantities provided as a context and are not used anywhere in our calculations, which are all exact using the superlattice single-particle cosine potentials  $V(x)$  and the inter-particle  $1/x$  Coulomb interaction  $V_{ij}$ .

In Fig. 1, we present the exactly calculated noninteracting band structure of the 1D superlattice for different values of  $m$ , clearly showing an exponential flattening of the bands with increasing  $M$ . Some representative non-interacting Wannier functions are also shown to emphasize the almost ‘localized’ nature of the noninteracting superlattice band states for  $m = 1.4$  ( $M = 7$ ) and  $1.6$  ( $M = 8$ ). Thus, impressive band flattening is already achieved for a modest incommensuration of  $m = 1.4$  or  $1.6$ .

In Fig. 2, we show the calculated density distributions in the interacting moiré case ( $M = 7, 8$ ) compared with the corresponding noninteracting situations for  $N_e = 5$ . It is obvious that while all sites have finite occupancies in the noninteracting situation (there are  $63/M$  sites in the moiré system) indicating a standard metallic band, the

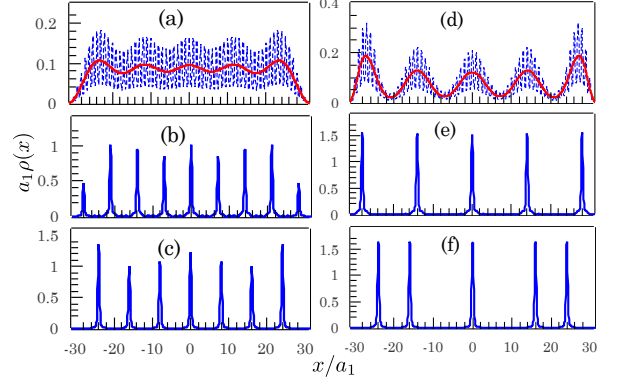


Figure 2. Spatial density distribution for 5 non-interacting electrons in a lattice field with (a)  $M = 1$ , (b)  $M = 7$ , (c)  $M = 8$ . (d)-(f): interacting counterpart of (a), (b) and (c), respectively. The red lines are smoothed functions of the actual density distributions (dashed lines).

corresponding interacting situation is strongly localized with only 5 density peaks corresponding to the 5 particles in the system. For comparison, we also show the results for the original lattice ( $M = 1$ ), where the localization is substantially weaker than for  $M = 7, 8$  showing the strong enhancement of correlation effects in the interacting superlattice system. The corresponding dimensionless interaction strengths, as obtained from our calculated band widths, increase from  $V_c/t = 2.5$  for  $M = 1$  to  $123.6$  ( $M = 7$ ) and  $618.8$  ( $M = 8$ ). Clearly, the moiré superlattice enables the manifestation of the localized insulating correlated states in a generic manner.

In Fig. 3, we show that the correlation physics in the superlattice is much more akin to Mott localization [9] (i.e. driven by  $V_c/t$  with narrow band physics of a small  $t$  playing the decisive role) than Wigner crystallization [10] (i.e. driven by increasing  $r_s$ , the dimensionless density of the system). Changing  $r_s$  from 1 to 10 does not change the density profile at all for the interacting superlattice ( $M = 8$ ), but it affects the density profile in the original lattice ( $M = 1$ ) as indeed it should since increasing  $r_s$  enhances  $V_c/t$  from a smaller value to a larger one (by contrast, the superlattice already has exponentially high  $V_c/t$ ).

In Fig. 4, we show the calculated charge gap  $\Delta(N_e) = E(N_e + 1) + E(N_e - 1) - 2E(N_e)$  for different  $M (= 1, 3, 7, 8)$  values plotted as a function of the electron number (or equivalently, band filling), clearly showing that a correlated insulating gap emerges in the superlattice (for  $M = 7, 8$ ) where the corresponding non-superlattice case ( $M = 1, 3$ ) does not manifest any pronounced insulating behavior. The overall smooth increase of the gap with  $N_e$  is the so-called collective Coulomb blockade behavior where the gap increases smoothly in any finite system as the number of electrons increases in it because of the standard Coulomb repulsion physics [11, 12]. The real

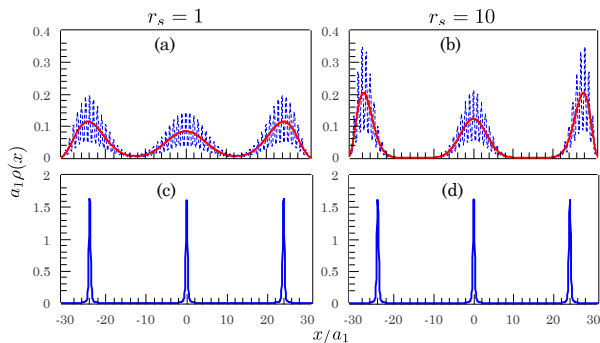


Figure 3. Density-induced localization in 3-electron systems from  $r_s = 1$  ((a) and (c)) to  $r_s = 10$  ((b) and (d)). (a)-(b): Original lattice potential  $M = 1$  with  $V_c/t = 2.5$  and  $25$  for  $r_s = 1$  and  $10$  respectively. The red lines are smoothed functions of the actual density distributions (dashed lines). (c)-(d): Incommensurate lattice potential  $M = 8$  with  $V_c/t = 618.8$  and  $6188$  for the two values of  $r_s$ .

correlated gaps of interest are the peaks (at half-filling for  $M = 7, 8$ ) above the smooth background, and one should subtract out the smooth background to get the true correlated gap. The moiré system manifests a large correlated gap at the commensurate filling of  $1/2$  (and in fact, there are smaller gaps at other commensurate filling such as  $1/3$  also, but severe finite size effects overwhelm those gaps in the results of Fig. 4). Note that while this correlated gap arises for  $m = 1.4$  ( $M = 7$ ) and  $m = 1.6$  ( $M = 8$ ), it is manifestly absent at the intermediate  $m$ -value of  $1.5$  ( $M = 3$ ). This is a clear indication of the interplay between moiré superlattice and Coulomb interaction – the  $M = 3$  ( $m = 1.5$ ) case has very weak band flattening effect, and hence very weak correlation gap.

The manifestation of correlated gap is nonmonotonic in the value of  $m$ , it is enhanced when  $m$  approaches an irrational such as  $\sqrt{2} \sim 1.414\dots$  and Golden mean  $\sim 1.618\dots$  for  $m = 1.4$  and  $1.6$  respectively because the rational approximation to such irrationals involves a large value of  $M$ , concomitantly flattening the single-particle bands exponentially, and hence enhancing the dimensionless coupling strength  $V_c/t$  very strongly. This does not happen at the simple rational fraction  $m = 1.5 = 3/2$  (i.e.  $M = 3$ ) where the band flattening and hence the insulating gap effects are weak. We believe this same phenomenon is reflected in 2D moiré superlattices where the correlated insulating gaps are fragile because the twist angle  $\theta$  varies somewhat over the sample size, and sometimes it simply produces rational bands without enhancing the correlation effects.

In this context, we discuss a subtle competition, shown in Fig. 5, between aperiodic incommensuration and interaction, which reflects the delicate fragility of the correlated insulator phase. While the incommensuration physics discussed above originates from the localized bulk Wannier wavefunctions, the “aperiodic” fragility de-

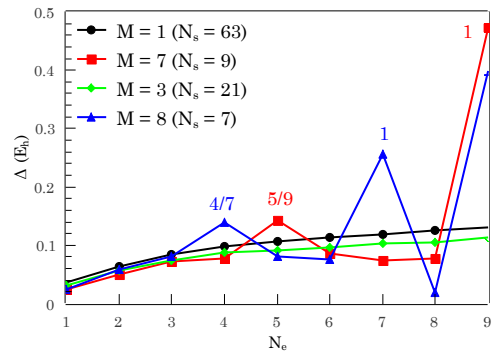


Figure 4. Charge gap as a function of the electron number  $N_e$  for lattice potentials with various degrees of incommensuration. Some filling factors  $N_e/N_s$  are indicated with  $N_s$  being the number of moiré sites.

pends on the finite system size (or the boundary). This physics arises from the incommensurate system with a very large  $M$  potentially having a unit cell size  $A$  exceeding the system size. We ask what happens if we change the bichromatic incommensuration by slightly modifying  $a_2 = 1.4a_1$  to  $a_2 = 1.405a_1$  (i.e. change  $m$  by less than 1% from  $1.4$  to  $1.405$ ) keeping everything else exactly the same. With such fine tuning, e.g from  $m = 1.4$  to  $1.403$ ,  $M$  increases from  $7$  to  $1403$ ! Since this period,  $A = 1403a_1$ , is much larger than the system size, the system is now aperiodic and may undergo uncorrelated incommensurate localization [6, 7, 13]. In Figs. 5(a)-(c), the number of occupied moiré sites changes from  $3$  to  $5$  as  $m$  increases from  $1.4$  to  $1.403$ , then reverts back to  $3$  but occupying different spatial locations when  $m$  reaches  $1.405$ . The way to circumvent this incommensuration-induced physics and revive strong correlation effects is to increase the basic interaction strength by increasing  $r_s$ , as shown in Figs. 5(d)-(f), where for  $r_s = 4$ , the same tuning of  $m$  has no effect on the correlated insulator phase. As the correlated insulating phase minimizes the interaction energy, we show the calculated  $\langle V_{ij} \rangle / r_s$  in Fig. 5(g) with continuously varying  $m$ . Starting with  $a_2 = 1.4a_1$ , where the correlated insulator clearly exists, and going to  $a_2 = 1.5a_1$ , the rational approximation to  $m = a_2/a_1$  varies making  $M$  sometimes very large and sometimes rather small, consequently almost randomly suppressing (the peaks in Fig. 5(g)) and enhancing the correlation effects. For larger  $r_s$  ( $r_s = 4$ ), this incommensuration-induced fragility is less prominent because interaction now overcomes incommensuration. We believe that the observed fragility of the correlated insulator phase in tBLG and related moiré systems may be related to this competition between aperiodic incommensuration and interparticle interaction as shown in Fig. 5.

One direct way to control the Coulomb coupling is by using an external gate to screen the interaction as already demonstrated in tBLG [14–16]. In Fig. 6, we show the ef-

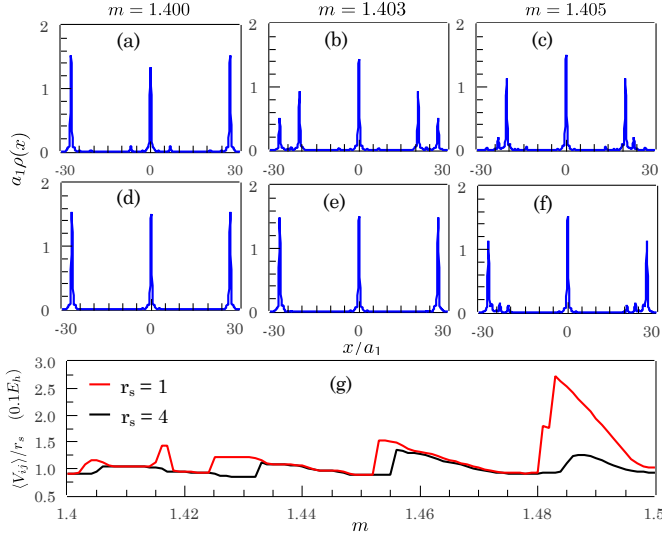


Figure 5. Competition between the interaction and fine-tuning-induced localization in the 3-electron system by slightly varying  $m$ . (a)-(c): A system with  $r_s = 1$  undergoes significant adjustment as  $m$  increases. (d)-(f): A system with higher  $r_s = 4$  shows only minor changes as  $m$  increases. (g) Small values of the calculated average interaction energy normalized by  $r_s$ , as a function of the lattice commensuration  $m$ , indicating correlated insulating phases whereas the peaks indicating the absence of correlated insulator.

fects of external screening by a gate placed at a distance of  $D$  so that the screened Coulomb interaction between 2 electrons separated by a distance  $x$  gets suppressed to  $x^{-3}$  for  $D \ll x$  instead of the usual  $1/x$  dependence. Since the period  $A (Ma_1) \gg a_1$  controls the moiré length scale, the gating effect is strong in the moiré system for  $D < A$ . This can be clearly seen in Fig. 6 where we show the calculated density distribution for  $M = 7$  and 8, which, for small  $D = a_1$ , becomes essentially metallic with all sites manifesting occupancy as in the weakly interacting system. The corresponding charge gap enhancement (not shown) also disappears, thus the correlated insulator phase can be suppressed by gating, as seen in recent tBLG experiments [14–16].

Before concluding, we mention our approximations. We consider spinless electrons because our focus is on the charge physics, but we verified that our conclusions do not change at all if we include spin since the exchange energy in the insulating phase is exponentially small with spin playing no role on the physics of gaps and density distributions of interest to us. This is demonstrated in Fig. 7 where we diagonalize equivalent tight-binding models for spinful and spinless 1D interacting systems where the hopping strength is  $t$ , the intersite interaction is  $V_c/|j-i|$  and the on-site potential is  $2V_c$  ( $V_c$  and  $t$  are obtained from the continuum model). It is clear that our results presented in this work are unaffected by the spinless approximation. We cannot, however, com-

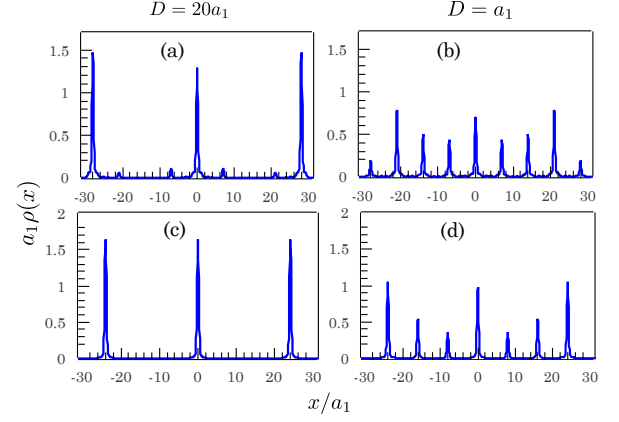


Figure 6. Screening-induced delocalization for 3-electron systems from the screening length  $D = 20a_1$  ((a) and (c)) to  $D = a_1$  ((b) and (d)). (a)-(b): Lattice potential with  $M = 7$ ,  $V_c/t = 82.8$  and  $1.2$  for  $D/a_1 = 20$  and  $1$ . (c)-(d): Lattice potential with  $M = 8$ ,  $V_c/t = 389.0$  and  $4.8$  for the two values of  $D$ .

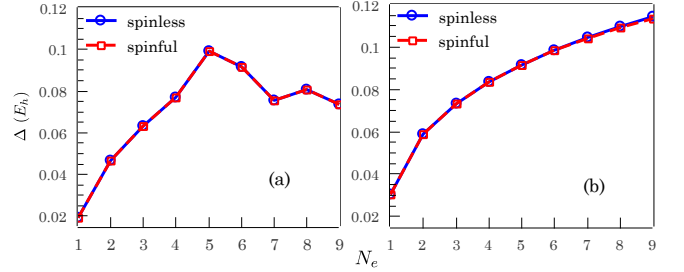


Figure 7. Charge gap calculated from interacting spinless and spinful tight-binding models. (a) Superlattice  $M = 7$  with 10 sites,  $V_c = 1/7 E_h$ ,  $t = 1.2 \times 10^{-3} E_h$ . (b) Original lattice  $M = 1$  with 70 sites,  $V_c = 1 E_h$ ,  $t = 0.4 E_h$ . In both cases, the exchange energy difference between the spinful and spinless models is negligible.

ment on the magnetic properties of tBLG and related 2D moiré systems based on our work. We also cannot discuss topological properties of 2D moiré systems based on our work since we have only included the competition between incommensuration and interaction, and have not incorporated any topology in our model. Our finite size calculation has the advantage of being exact, and thus our qualitative conclusions should apply quite generally, but obviously we cannot estimate the quantitative details of any 2D moiré system. Our work should, however, apply directly to 1D bichromatic lattices [5–8].

*Conclusion* - We have carried out finite-size exact calculations for interacting 1D bichromatic lattices, showing that correlated insulating states manifest generically when the moiré superlattice has a large unit cell (e.g.  $m = 1.4$  and  $1.6$ ) compared with the original lattice, but not when the two lattices are almost commensurate (e.g.  $m = 1.5$ ). We also find that very slight tuning of the period of the second lattice may drastically suppress the in-

ulating phase in finite systems because such tuning may drive the moiré system from being a superlattice with a large period to a finite disordered system. We speculate that our findings qualitatively explain several features of the correlated insulating phase in 2D moiré systems including gate-induced suppression of the insulator and the generic fragility of the insulating phase.

*Acknowledgement* - This work is supported by the Laboratory for Physical Sciences.

- 
- [1] Y. Cao, V. Fatemi, S. Fang, K. Watanabe, T. Taniguchi, E. Kaxiras, and P. Jarillo-Herrero, *Nature* **556**, 43 (2018).
  - [2] Y. Cao, V. Fatemi, A. Demir, S. Fang, S. L. Tomarken, J. Y. Luo, J. D. Sanchez-Yamagishi, K. Watanabe, T. Taniguchi, E. Kaxiras, R. C. Ashoori, and P. Jarillo-Herrero, *Nature* **556**, 80 (2018).
  - [3] M. Yankowitz, S. Chen, H. Polshyn, Y. Zhang, K. Watanabe, T. Taniguchi, D. Graf, A. F. Young, and C. R. Dean, *Science* **363**, 1059 (2019), 1808.07865.
  - [4] X. Lu, P. Stepanov, W. Yang, M. Xie, M. A. Aamir, I. Das, C. Urgell, K. Watanabe, T. Taniguchi, G. Zhang, A. Bachtold, A. H. MacDonald, and D. K. Efetov, *Nature* **574**, 653 (2019).
  - [5] M. Schreiber, S. S. Hodgman, P. Bordia, H. P. Lüschen, M. H. Fischer, R. Vosk, E. Altman, U. Schneider, and I. Bloch, *Science* **349**, 842 (2015), 1501.05661.
  - [6] X. Li, X. Li, and S. Das Sarma, *Phys. Rev. B* **96**, 085119 (2017).
  - [7] H. P. Lüschen, S. Scherg, T. Kohlert, M. Schreiber, P. Bordia, X. Li, S. Das Sarma, and I. Bloch, *Phys. Rev. Lett.* **120**, 160404 (2018).
  - [8] T. Kohlert, S. Scherg, X. Li, H. P. Lüschen, S. Das Sarma, I. Bloch, and M. Aidelsburger, *Phys. Rev. Lett.* **122**, 170403 (2019).
  - [9] N. F. Mott, *Proc. Phys. Soc. Sect. A* **62**, 416 (1949).
  - [10] E. Wigner, *Phys. Rev.* **46**, 1002 (1934).
  - [11] C. A. Stafford and S. Das Sarma, *Phys. Rev. Lett.* **72**, 3590 (1994).
  - [12] T. Hensgens, T. Fujita, L. Janssen, X. Li, C. J. Van Diepen, C. Reichl, W. Wegscheider, S. Das Sarma, and L. M. Vandersypen, *Nature* **548**, 70 (2017), 1702.07511.
  - [13] S. Das Sarma, S. He, and X. C. Xie, *Phys. Rev. Lett.* **61**, 2144 (1988).
  - [14] P. Stepanov, I. Das, X. Lu, A. Fahimniya, K. Watanabe, T. Taniguchi, F. H. L. Koppens, J. Lischner, L. Levitov, and D. K. Efetov, “The interplay of insulating and superconducting orders in magic-angle graphene bilayers,” (2019), arXiv:1911.09198.
  - [15] Y. Saito, J. Ge, K. Watanabe, T. Taniguchi, and A. F. Young, *Nat. Phys.*, 1 (2020).
  - [16] X. Liu, Z. Wang, K. Watanabe, T. Taniguchi, O. Vafek, and J. I. A. Li, “Tuning electron correlation in magic-angle twisted bilayer graphene using Coulomb screening,” (2020), arXiv:2003.11072.